

Orexin (also known as hypocretin) neurons, located in the hypothalamus, promote arousal and consolidate wakefulness. Organisms without functioning orexin neurons show elements of the narcolepsy phenotype in humans (Sakurai, 2007). To complement the ongoing experimental characterization of orexin neurons, we developed a mathematical model of these cells. A model will allow a more detailed investigation of cell dynamics without some of the limitations of experimental work. In this paper, we describe a Hodgkin-Huxley model developed to study the currents and interactions of orexin neurons. Basing its foundation on the Hodgkin-Huxley models for currents, the model brings together the currents perceived to be present in orexin neurons.

Previous experimental work has identified evidence for seven currents ( $i_{Na}$ ,  $i_K$ ,  $i_{K2}$ ,  $i_h$ ,  $i_{CAN}$ ,  $i_T$ , and  $i_{Cal}$ ) that contribute to the properties of orexin neurons. In addition to these currents, we also included a general leak current. A fast sodium current,  $i_{Na}$ , causes spiking by drawing up the membrane potential to a high level of depolarization (Li et al; 2002), (Hoang et al; 2003). When the neuron is depolarized, a fast-inactivating potassium current,  $i_K$ , activates to send the electrical potential down into a hyperpolarization regime (Hoang et al; 2003). A slowly inactivating potassium current,  $i_{K2}$ , which is found in thalamocortical neurons, shapes the spike by pulling it down after its peak and slowly inactivating to affect the frequency of spiking in the model (McCormick, Huguenard; 1992). There is also a hyperpolarization-activated current,  $i_h$ , that draws the potential back into the regime of spiking; this results in a “sag” during appropriate hyperpolarization protocols (Eggermann et al., 2003), (Hoang et al; 2003).

Based on the research of Eggermann et al. (2003), there exists a nonspecific cation current,  $i_{CAN}$  in orexin neurons that is calcium-dependent and assists in depolarization and spike shape. It is enhanced by  $i_T$ , a low-voltage-activated (LVA) calcium current (McCormick, Bal; 1997). In addition to  $i_T$ , a calcium leak current,  $i_{Cal}$ , provides a source of calcium for  $i_{CAN}$  that persists when voltage-activated calcium currents are blocked (Eggermann et al; 2003).

However,  $i_{CAN}$  is a challenge to investigate experimentally due to the absence of the necessary selective antagonists. Therefore, we have developed a novel Hodgkin-Huxley model for an orexin neuron to investigate the properties of  $i_{CAN}$  in a theoretical framework.

## METHODS:

To develop the model, we used a standard Hodgkin-Huxley model formalism consisting of an equation for voltage in summed current notation and equations describing the dynamics of the current gating variables. The respective currents followed models of differential equations with gating variables of activation and inactivation depending on the current. The equation for voltage in summed current notation:

$$dv/dt = (I_0 - i_{Na}(v) - i_K(v) - i_h(v) - i_{K2}(v) - i_T(v, [Ca^{2+}]) - i_{CAN}(v) - i_l(v) - i_{Cal}(v, [Ca^{2+}]))/c$$

$$i_{Na}(v) = g_{na} * h * (v - v_{na}) * m^3$$

$$i_K(v) = g_k * (v - v_k) * n^4$$

$$i_h(v) = g_h * r * (v - v_h)$$

$$i_T(v, [Ca^{2+}]) = p_{ca} * m^2 * h_t * (v - v_{ca}([Ca^{2+}])))$$

$$\begin{aligned}
i_{\text{CAN}}(v) &= g_{\text{can}} * z^2 * (v - v_{\text{can}}) \\
i_{\text{K2}}(v) &= (m_{\text{k2a}} * h_{\text{k2a}} * (v - v_{\text{k}}) * g_{\text{maxk2a}} + m_{\text{k2b}} * h_{\text{k2b}} * (v - v_{\text{k}}) * g_{\text{maxk2b}}) \\
i_{\text{l}}(v) &= g_{\text{l}} * (v - v_{\text{l}}) \\
i_{\text{Cal}}(v, [\text{Ca}^{2+}]) &= g_{\text{cal}} * (v - v_{\text{ca}}([\text{Ca}^{2+}])) \\
v_{\text{ca}}([\text{Ca}^{2+}]) &= (RT/2F) * 1000 * \ln(13000 / [\text{Ca}^{2+}]) \\
\text{and } c &= 1
\end{aligned}$$

$$\begin{aligned}
dc_{\text{ac}}/dt &= (-300 * (i_{\text{T}}(v, c_{\text{ac}}) + i_{\text{Cal}}(v, c_{\text{ac}})) - 360 * c_{\text{ac}} + 360 * c_{\text{a0}}) \\
i_{\text{T}}(v, c_{\text{ac}}) &= p_{\text{ca}} * m_{\text{t}}^2 * h_{\text{t}} * (v - v_{\text{ca}}(c_{\text{ac}}))
\end{aligned}$$

Table 1: Parameters for Current Equations

Conductance	Maximum Conductance ( $\mu\text{S}$ )	Reversal Potential (mV)
$i_{\text{Na}}$	$g_{\text{na}}=290$	$v_{\text{na}}=50$
$i_{\text{K}}$	$g_{\text{k}}=20$	$v_{\text{k}}=-77$
$i_{\text{h}}$	$g_{\text{h}}=0.037$	$v_{\text{h}}=-10$
$i_{\text{K2}}$	$g_{\text{maxk2a}}=16, g_{\text{maxk2b}}=10$	$v_{\text{k}}=-77$
$i_{\text{l}}$	$g_{\text{l}}=0.3$	$v_{\text{l}}=-54.4$
$i_{\text{CAN}}$	$g_{\text{can}}=3$	$v_{\text{can}}=-20$
$i_{\text{T}}$	$p_{\text{ca}}=3$	$v_{\text{ca}}(\text{Ca}^{2+})$
$i_{\text{Cal}}$	$g_{\text{cal}}=0.3$	$v_{\text{ca}}(\text{Ca}^{2+})$

Each gating variable is governed by a differential equation written in the form

$$d\mathbf{i}/dt = (\mathbf{i}_{\infty}(\mathbf{v}) - \mathbf{i}) / \tau_{\mathbf{i}}(\mathbf{v}) \quad (\text{equation 1})$$

with  $i_{\infty}(v)$  controlling the activation/inactivation of the variable and  $\tau_{\mathbf{i}}(v)$  controlling the speed of change of the current.

#### *Transient Sodium Current, $i_{\text{Na}}$ (Ermentrout, 2002)*

This current is the main one responsible for spiking in the neuron. It has two gating variables,  $m$  and  $h$ , that control activation and inactivation respectively. The equations for  $i_{\text{Na}}$  are:

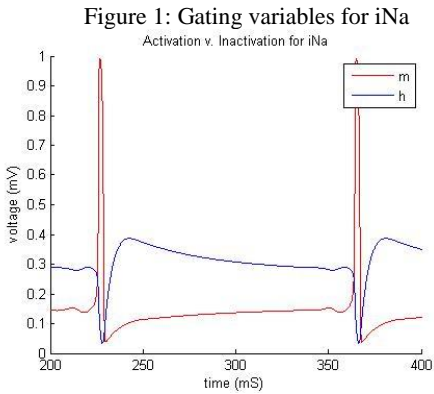
#### *Activation ( $m$ )*

$$\begin{aligned}
m_{\infty}(v) &= (.1 * (v + 40) / (1 - \exp(-(v + 40) / 10))) / ((.1 * (v + 40) / (1 - \exp(-(v + 40) / 10))) + 4 * \exp(-(v + 65) / 18)) \\
\tau_m(v) &= ((.1 * (v + 40) / (1 - \exp(-(v + 40) / 10))) + 4 * \exp(-(v + 65) / 18))^{-1}
\end{aligned}$$

#### *Inactivation ( $h$ )*

$$\begin{aligned}
h_{\infty}(v) &= (.07 * \exp(-(v + 65) / 20)) / (.07 * \exp(-(v + 65) / 20) + 1 / (1 + \exp(-(v + 35) / 10))) \\
\tau_h(v) &= (.07 * \exp(-(v + 65) / 20) + 1 / (1 + \exp(-(v + 35) / 10)))^{-1}
\end{aligned}$$

The neuron is able to spike due to the difference in speeds of activation and inactivation:  $\tau_m(v)$  is smaller than  $\tau_h(v)$  at the beginning of the spike, so  $m$  activates more quickly than  $h$  inactivates, and the spike occurs.



*Depolarization-Activated Potassium Current, iK (Ermentrout, 2002)*

The potassium current is activated by its gating variable,  $n$ , at depolarized levels attained by the membrane during a spike. The active current pulls the membrane potential back down to terminate the spike.

*Activation ( $n$ )*

$$n_{\infty}(v) = .01*(v+55)/(1-\exp(-(v+55)/10))/(.01*(v+55)/(1-\exp(-(v+55)/10))+.125*\exp(-(v+65)/80))$$

$$\tau_n(v) = (.01*(v+55)/(1-\exp(-(v+55)/10))+.125*\exp(-(v+65)/80))^{-1}$$

*Slowly-Inactivating Potassium Current, iK2 (Huguenard, McCormick ; 1992)*

This current, activated at negative voltages, helps keep the potential down. There are two parts to the current with separate activation and inactivation dynamics:

*Activation ( $mk2a, mk2b$ )*

$$mk2a, b_{\infty}(v) = 1/(1+\exp(-(v+43)/17))$$

$$\tau_{mk2a, b}(v) = 1/(\exp((v-81)/25.6)+\exp(-(v+132)/18))+9.9$$

*Inactivation ( $hk2a, b$ )*

$$hk2a, b_{\infty}(v) = 1/(1+\exp((v+58)/10.6))$$

$$\tau_{hk2a}(v) = 1/(\exp((v-1329)/200)+\exp(-(v+130)/7.1))+120$$

$$\tau_{hk2b}(v) = \tau_{hk2a}(v)*\text{heav}(-70-v)+8900*\text{heav}(v+70)$$

The dynamics of iK2 are unusual the current is the sum of two currents with slightly different dynamics in their  $\tau$  functions. These separate tau's cause the current to function at varying rates depending on the voltage.

*Hyperpolarization-Activated Current, ih (Buchholtz et al; 1992)*

ih activates at hyperpolarized potentials and is a strong current that allows the cell to recover from hyperpolarization by pulling the membrane back up to threshold. Its dynamics are such that it is only active when  $v < -80\text{mV}$ , so it is inactive during the normal spiking regime.

*Activation ( $r$ )*

$$r_{\infty}(v) = 1/(1+\exp((v+70)/7))$$

$$\tau_r(v) = 3/(1+\exp(-(v+110)/13))$$

### *Nonspecific Cation Current, iCAN*

Eggermann et al. (2003) hypothesize that there exists a calcium-dependent cation current that helps pull the potential up into a spiking regime. We modeled this current with a calcium-dependent activation variable,  $z$ , similar to the iCAN current described by Destexhe and Sejnowski (1993), but we modified the steady-state activation and time constant of  $z$  to fit the calcium concentrations present in our model.

#### *Activation ( $z$ )*

$$z_{\infty}([\text{Ca}^{2+}]) = .5 + .5 * \tanh(0.01 * ([\text{Ca}^{2+}] - 38))$$
$$\tau_z([\text{Ca}^{2+}]) = (20 * ([\text{Ca}^{2+}])^2 + 0.002)^{-1}$$

### *Low Voltage-Activated Calcium Channel, iT (Huguenard, McCormick; 1992)*

This reversal potential of this current is based on the concentration of calcium in the cell, but its gating variables are voltage-dependent. It has both activation and inactivation dynamics.

#### *Activation ( $mt$ )*

$$m_{\infty}(v) = 1 / (1 + \exp(-(v+70)/4))$$
$$\tau_{mt}(v) = (10,000) / (\exp(-(v+10)/10) + \exp((v+90)/6))$$

#### *Inactivation ( $ht$ )*

$$h_{\infty}(v) = 1 / (1 + \exp((v+70)/5))$$
$$\tau_{ht}(v) = (15,000)(22.7 + .27) / (\exp((v+48)/4) + \exp((v+407)/50))$$

### *General Leak Current, iI*

This leak current is a simple equation to account for natural inefficiency of the cell. It does not involve activation or inactivation variables.

### *Calcium Leak Current, iCal*

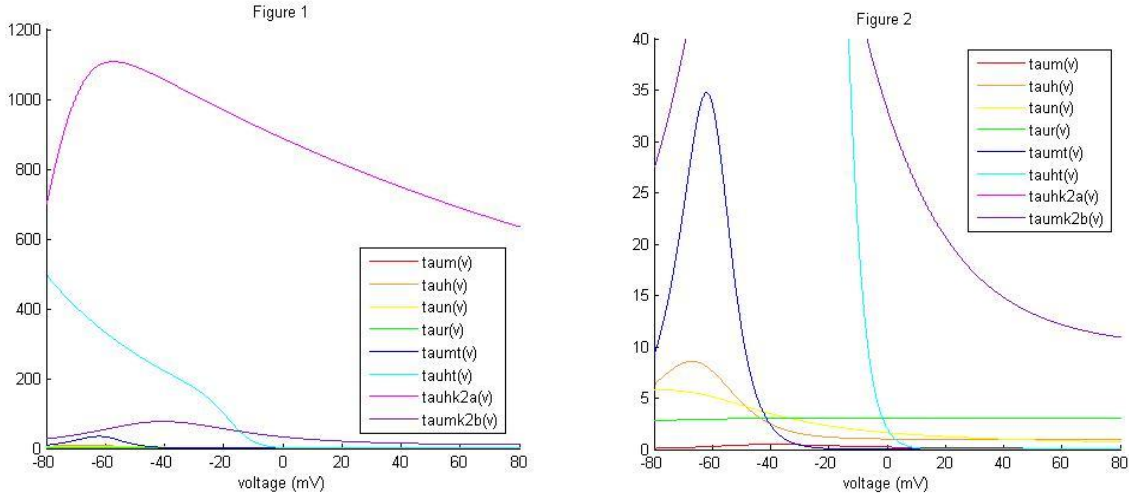
The currents that rely on calcium concentration need a source of calcium to function. This calcium can either come from voltage-dependent or -independent calcium currents or from internal stores of calcium in the environment of the cell. Experiments suggest that iT contributes to ICAN activation, but the hypothesized participation of ICAN in depolarizing the resting membrane potential continues when voltage-dependent calcium currents are blocked (Eggermann et al; 2003). Therefore, we included a calcium leak current to provide calcium for ICAN. We also compared the results obtained with iCal to results obtained with intracellular calcium concentrations modeled as increasing at a constant rate, consistent with constant release from intracellular stores.

### *Partitioning*

In order to better understand the currents acting on the membrane potential in different voltage regimes, we partitioned the currents in the neuron according to the magnitude of their tau functions. The partitions determined sets of tau functions acting on a similar time scale in a given region. These similar functions were studied together while the functions much larger were approximated as constant functions in that partition and the small tau functions were deemed approximately zero in that regime (instantaneous). When the tau function is assumed to be instantaneous, the gating variable is equal to its steady state activation function because there

is no delay that the tau function would otherwise have caused. The partitioning reveals the most active currents during hyperpolarization, in the interspike interval, and at depolarized voltages during the spike.

Figure 2: Tau Functions for Partitioning



The figures above depict the changes in the different currents during a spike.

Table 2: Partitions

Partition	Small tau's $\rightarrow i=i_s(v)$	Large tau's $\rightarrow i=constant$	Medium	Graph
-80 to -60	<ul style="list-style-type: none"> <li>▪ tauh(v)</li> <li>▪ taun(v)</li> <li>▪ taur(v)</li> <li>▪ taum(v)</li> </ul>	<ul style="list-style-type: none"> <li>▪ tauhk2b(v)</li> <li>▪ tauht(v)</li> </ul>	<ul style="list-style-type: none"> <li>▪ taumk2a(v) = (27,55)</li> <li>▪ taumt(v) = (10,30)</li> </ul>	Interspike Interval
-60 to -45	<ul style="list-style-type: none"> <li>▪ taum(v)</li> </ul>	<ul style="list-style-type: none"> <li>▪ tauhk2b(v)</li> <li>▪ tauht(v)</li> </ul>	<ul style="list-style-type: none"> <li>▪ taumk2a(v) = (55,75)</li> <li>▪ taumt(v) = (35,7)</li> <li>▪ tauh(v) = (7.7,4.5)</li> <li>▪ taun(v) = (5,4.5)</li> <li>▪ taur(v) = 3</li> </ul>	Hyperpolarization
-45 to 0	<ul style="list-style-type: none"> <li>▪ tauh(v)</li> <li>▪ taur(v)</li> <li>▪ taumt(v)</li> <li>▪ taun(v)</li> <li>▪ taum(v)</li> </ul>	<ul style="list-style-type: none"> <li>▪ tauhk2b(v)</li> </ul>	<ul style="list-style-type: none"> <li>▪ tauht(v) = (250,2)</li> <li>▪ taumk2a(v) = (85,33)</li> </ul>	Spiking Regime
0 to 40	<ul style="list-style-type: none"> <li>▪ taur(v)</li> <li>▪ tauht(v)</li> <li>▪ tauh(v)</li> <li>▪ taum(v)</li> <li>▪ taun(v)</li> <li>▪ taumt(v)</li> </ul>		<ul style="list-style-type: none"> <li>▪ taumk2a(v) = (33,19)</li> <li>▪ tauhk2b(v) = (900,800)</li> </ul>	Peak of Spike
40 to 80	<ul style="list-style-type: none"> <li>▪ taum(v)</li> <li>▪ taumt(v)</li> <li>▪ tauht(v)</li> </ul>	<ul style="list-style-type: none"> <li>▪ tauhk2b(v)</li> </ul>	<ul style="list-style-type: none"> <li>▪ taumk2a(v) = (15,12)</li> <li>▪ taur(v) = (3,3)</li> <li>▪ tauh(v) = (1,1.01)</li> <li>▪ taun(v) = (1,0.75)</li> </ul>	Depolarization

## RESULTS:

Our preliminary Hodgkin-Huxley-type model orexin neurons reproduced several important features of orexin neuron electrophysiology.

### *Intrinsic properties of model orexin neuron*

One characteristic of orexin neurons that started off the model was their spontaneous activity. The neuron reportedly spikes spontaneously at a rate of 3-4 Hz (Li et al; 2002), which would be in response to the depolarized resting membrane potential and the interactions between the various currents in the cell. The resting membrane potential of  $v = -57$  mV in the model neuron was consistent with that reported from orexin neuron slice recordings (Li et al., 2002). Other groups have reported even more depolarized resting membrane potentials for orexin neurons (Eggermann et al., 2003). However, we found that the model neuron's ability to spike at high resting membrane potentials was very sensitive to the activation and inactivation profiles of the  $\text{Na}^+$  current. As in experimental reports, the resting membrane potential for the model was determined by blocking  $i_{\text{Na}}$  (setting  $g_{\text{Na}}$  to zero), and observing the activity of the neuron. The currents that contributed to the resting membrane potential included  $i_{\text{Na}}$ ,  $i_{\text{CAN}}$ ,  $i_{\text{Cal}}$ ,  $i_{\text{T}}$ , and  $i_{\text{K2}}$ .  $i_{\text{K}}$  activates at depolarized levels, and  $i_{\text{h}}$  is active at hyperpolarized levels, so neither is working at the resting membrane potential.  $i_{\text{Na}}$ ,  $i_{\text{K2}}$ ,  $i_{\text{CAN}}$ ,  $i_{\text{Cal}}$  all bring the potential up, while  $i_{\text{K2}}$  and  $i_{\text{T}}$  push the potential down.

When studying experimental results on orexin neurons, we found a discrepancy in the resting membrane potential that was significant, though the results that varied had similar intrinsic firing rates nonetheless. The resting membrane potential of this model falls in line with that of Li et al. (2002) at  $v = -57$  mV. In the studies by Eggermann et al. (2003), the resting membrane potential was  $-45.6$  mV, but with the dynamics of our  $i_{\text{Na}}$  and  $i_{\text{K}}$ , spiking in this regime was impossible due to depolarization block. The point of half-activation for  $i_{\text{Na}}$  falls at  $-45$  mV, with full activation around  $0$  mV. Various  $i_{\text{Na}}$  currents were studied with half activation falling between  $v = -42$  mV and  $v = -15$  mV. Ultimately, with the level of depolarization of the resting membrane potential, the  $i_{\text{Na}}$  current used in the model reflected these spiking dynamics.

The final resting membrane potential fell out from the interactions between  $i_{\text{Na}}$ ,  $i_{\text{CAN}}$ ,  $i_{\text{K2}}$  and  $i_{\text{l}}$ . As  $i_{\text{K}}$  and  $i_{\text{h}}$  are inactive until depolarized levels and  $i_{\text{h}}$  is only active and hyperpolarized levels, the other currents take over.

Figure 5: Spontaneous Activity

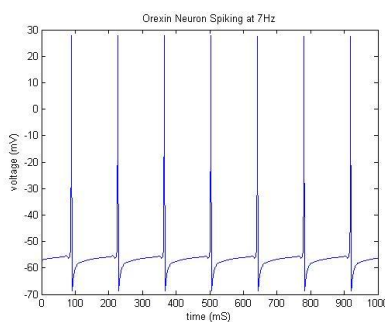


Figure 6: Model with Currents  
Model Spontaneously Spiking

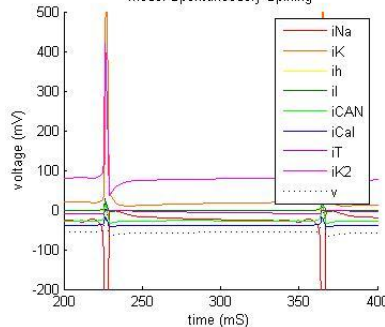
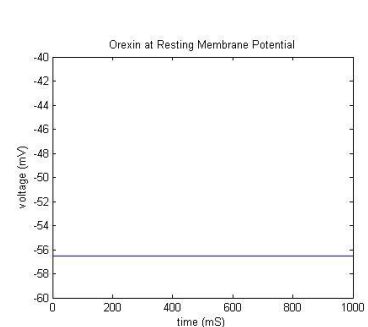


Figure 7: Resting Membrane Potential



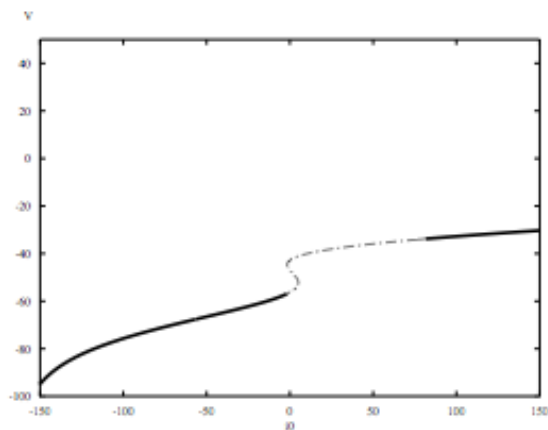
Based on experimental results, an orexin neuron spontaneously spikes with an average frequency of 3-4 Hz (Li et al; 2002) that suggests at least one slow current is involved in pulling the membrane potential up to the firing threshold. In the model orexin neuron, spiking occurs as a result of increasingly large subthreshold oscillations (STOs). These STOs are created by the interactions between  $i_{\text{Na}}$  and  $i_{\text{K2}}$ .  $i_{\text{Na}}$  pulls the potential up a bit, but  $i_{\text{K2}}$  pushes back toward hyperpolarization at the same time. This seesaw effect eventually results in a spike when  $v$  is

depolarized enough to enter the spiking regime. This mechanism is explained in more detail below.

### *Bifurcation structure of the model*

In order to better understand the dynamics of the model orexin neuron under different applied currents, we constructed a bifurcation diagram using  $i_0$  as our parameter. Consistent with bifurcation diagrams for other neuronal models, the voltage of the model orexin neuron goes to a steady state when the neuron is strongly hyperpolarized or depolarized. At  $i_0 = -1.7$ , the system undergoes a Hopf bifurcation and begins spiking. This allows the neuron to spike intrinsically (when  $i_0 = 0$ ). As  $i_0$  increases between 0 and 81.85, the regime is unstable and spiking continues at an increasing rate. When  $i_0$  hits 81.85, though, the neuron is too depolarized to continue spiking and enters a stable depolarized regime at a second Hopf Bifurcation.

Figure 10: Bifurcation Diagram



### *Model response to external stimuli*

In an experiment by Eggermann et al. (2003), three different experimental protocols were used to explore the intrinsic properties of orexin neurons in slice (Figure 3):

1. The neuron spontaneously spikes, and the frequency of spiking increases with a depolarizing pulse.
2. The neuron is hyperpolarized and then given a depolarizing pulse that allows it to spike after first producing a low-threshold spike.
3. The neuron is hyperpolarized to the point that even with a depolarizing current, it cannot produce a calcium spike.

We reproduced these protocols in our model orexin neurons and obtained similar behavior (Figure 4). A1 shows an increased spiking frequency, A2 has a low-threshold calcium spike, a sodium spike, and ADP, and A3 shows that additional hyperpolarization can prevent the LTS and ADP.

Figure 3

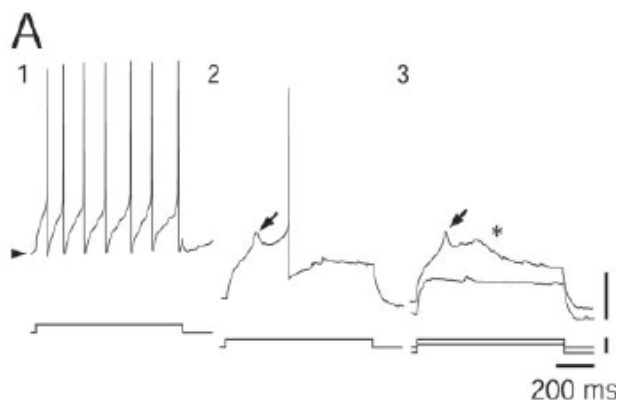


**Figure 1.** Characterization of neurons expressing Hcr/Ox or MCH. *A*<sub>1</sub>, Tonic firing in response to a depolarizing current pulse delivered from the level of resting potential (arrowhead). *A*<sub>2</sub>, *A*<sub>3</sub>, LTS (arrow) and ADP (asterisk) triggered by a depolarizing current pulse delivered from an hyperpolarized level. Additional hyperpolarization eliminates the LTS and the ADP (bottom trace in *A*). *B*, Superimposed responses to

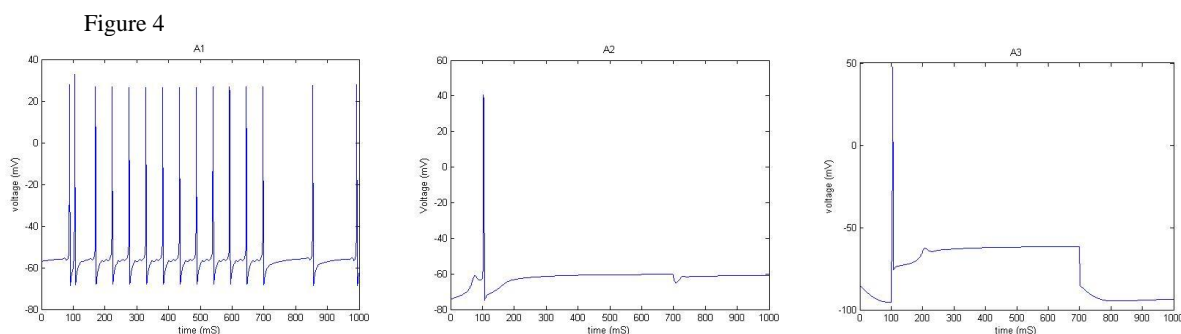


**Figure 4.** In *A*<sub>1</sub>, the model is given a pulse of 15mV from 100–700ms. The model spikes more quickly in response to this pulse. *A*<sub>2</sub> depicts a calcium spike and then one sodium spike with a sag after the spike in response to being hyperpolarized by -80mV and given a pulse of 23mV. *A*<sub>3</sub> shows the LTS and the recovery hyperpolarized by -140mV and with a pulse of 59mV.

Depolarizing current ( $i_0 = 50\text{mV}$ ) generates fast spiking in the neuron by pushing the neuron farther up into the spiking regime, shortening the time the neuron takes to recover from a spike and reach the spiking regime again. When a depolarizing current is applied to the model at a hyperpolarized level, calcium spikes are produced when the pull of  $i_{\text{CAN}}$  and  $i_{\text{T}}$  that are both activated by the applied current and drag the neuron up to its spiking regime.  $i_{\text{CAN}}$  is also responsible for the after depolarization (ADP) created under some conditions in this trial. When the neuron does not reach its spiking regime after a spike, ADP levels off the voltage.

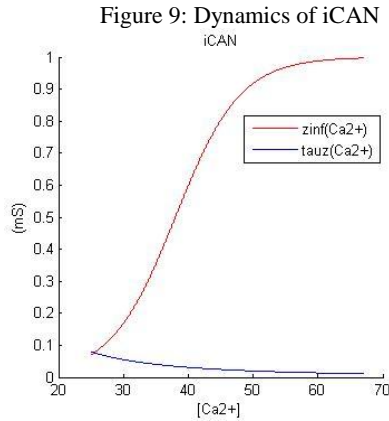
#### *i*CAN and calcium dynamics in the model

Eggermann and colleagues reported the presence of a calcium-dependent nonspecific current ( $i_{\text{CAN}}$ ) based on the presence of an ADP following the LTS, and they speculated that this current could contribute to the depolarized resting membrane potential of orexin neurons (Eggermann et al., 2003). We modeled intracellular calcium concentration as a combination of two active calcium-based currents,  $i_{\text{T}}$  and  $i_{\text{Cal}}$ . The calcium that  $i_{\text{Cal}}$  provides activates  $i_{\text{CAN}}$  to function initially in the model even when the voltage-based currents are turned off. In more hyperpolarized regimes,  $i_{\text{T}}$  activates and contributes even more calcium to  $i_{\text{CAN}}$  for further activity and ADP. In order to get the depolarized RMP we wanted in the neuron, we used the  $i_{\text{CAN}}$  to further depolarize the neuron at rest. We included  $i_{\text{CAN}}$  in our model orexin neuron,

and we chose the steady-state activation profile of its calcium-dependent gating variable,  $z$ , and time constant,  $\tau_{z}$ , to be consistent with these roles.

The  $z_{inf}$  function we chose for  $i_{CAN}$  encourages maximum activity as the potential increases into a spiking regime.  $i_{CAN}$  must be actively pulling the neuron potential into the spiking regime as the calcium concentration increases. The  $z_{inf}$  function, therefore, increases right away and stays near maximum levels throughout the calcium range

The  $\tau_{z}$  function we chose fits specifically with  $i_{CAN}$  because it enables the current to be almost instantaneous. The function of  $i_{CAN}$  is to depolarize the neuron into a spiking regime, so as the calcium concentration increases over its range,  $\tau_{z}$  makes  $i_{CAN}$  react faster to shifts in the neuron.



### *Partitioning helps identify mechanism for subthreshold oscillation*

Some dynamics appeared through the construction of the model that have not been reported experimentally. Subthreshold oscillations caused by the interactions of  $i_{Na}$  and  $i_{K2}$  help pull the slowly-spiking model up to a spike. Such results suggest canard behavior.

To better understand the role of each current during different parts of the spike, we partitioned the spike into 5 sub-regimes and studied the time courses of model variables during each sub-regime (see Figures 1 and 2, Table 2). In each regime, the currents whose tau functions took on values far larger than the other functions were deemed to approximately unchanging because the overall differential equations for the respective currents would be approximately zero when the tau function was approximately infinite. Similarly, the currents whose tau functions are very small compared to the other functions in the regime are approximately equal to their inf functions because the currents' differential equations are approximately infinite when the tau functions are approximately zero. Thus the currents that are changing in a given regime are the ones whose tau functions are on the same scale as the neighboring taus.

The results of the partitioning showed that in the interspike interval, the currents most active are likely  $i_T$  and  $i_{K2}$  because the inactivation taus of  $i_T$  and  $i_{K2}$  are among the largest functions in that regime and so are not inhibiting the current very much. In the hyperpolarized interval, the  $i_{Na}$ ,  $i_K$ , and  $i_h$  activation tau functions decrease and so the currents move into a faster regime that activates their respective currents. The inactivation gating variables of  $i_T$  and  $i_{K2}$  are still slow in the hyperpolarized regime, and the tau's for  $i_K$  and  $i_h$  are decreasing toward zero.  $\tau_{um}(v)$ , the tau function for the  $i_{Na}$  activation variable, is still very fast, and thus  $i_{Na}$  has the potential for becoming active very quickly. In the beginning of the spike, the currents involved in spiking are moving very quickly as would  $i_K$  and  $i_h$  if their respective  $inf(v)$  functions were active in this regime. The inactivation current for  $i_{K2}$  is still not working very

fast, though the inactivation current for  $i_T$  is speeding up through this interval. At the top of the spike, the activation tau function of  $i_{K2}$  is moving more quickly than the inactivation tau function allowing  $i_{K2}$  to remain active. The rest of the tau's are acting close to instantaneously in this regime. The depolarization regime shows that only  $i_{K2}$  is changing, and the tau functions that are shifting are the activation tau function for one part of  $i_{K2}$  and the inactivation tau function for the other  $i_{K2}$  variable.

The partitions have useful implications for the model of the neuron. Because  $i_{K2}$  and  $i_{Na}$  have tau functions that indicate the currents are active during the interspike interval, they likely control the potential in this regime. The positive reversal potential for  $i_{Na}$  causes it to pull the potential up. As the potential moves upward, though, it distances itself from  $i_{K2}$ 's negative reversal potential and thus  $i_{K2}$  pulls on the potential to get it back down. This pushing by  $i_{Ka}$  and, in turn, the pulling by  $i_{K2}$  could create the subthreshold oscillations observed in the interspike interval.

## DISCUSSION:

The model orexin neuron is based on Hodgkin Huxley-type modeling formalism and is consistent with several important properties of orexin neuron electrophysiology. Eight currents contribute to the overall neuron modeled, which has a resting membrane potential of  $-57\text{mV}$ , spikes spontaneously at 3-4Hz, and produces spikes of approximately  $80\text{mV}$ . The discrepancy we found in the resting membrane potential of orexin neurons in experimental results can be explained largely by the type of bath used. In this model, the resting membrane potential of  $-45$  causes depolarization block that prevents all neuron activity.

The spiking of the model follows closely to the experimentation of Eggermann et al. as the spike slowly draws upward into a realm of depolarization and then spikes once it reaches the spiking threshold. In our model, a sub-threshold oscillation involving  $i_{Na}$  and  $i_{K2}$  helps draw the potential up to threshold. This activity is consistent with a canard mechanism (Jalics et al, 2008).

### *Canards*

Canard trajectories define thresholds for neurons. Though very rare in nature, it is possible that a canard exists in neuron activity (Izhikevich, 1976). Canards function in oscillating systems that change by large amounts when perturbed by some parameter (Murray, 2002). Jalics and colleagues recently reported the involvement of a slow  $K^+$ -current in a canard-like mechanism for mixed-mode oscillations in a model of a neuron from entorhinal cortex. The sub-threshold oscillations in our model depend on  $i_{K2}$  and may reflect a similar mechanism. These oscillations are caused by the interactions between  $i_{Na}$  and  $i_{K2}$ , and they seem to assist in pulling the membrane potential up to a spiking regime. This canard structure could make the neuron more robust to noise and facilitate relatively slow intrinsic spiking.

### *Calcium Dynamics*

Calcium dynamics are important for the behavior of this model. Currents exist in the neuron that are calcium-dependent instead of voltage-dependent. The initial calcium currents in place failed to allow continued spiking of the neuron when calcium currents were turned off as in the experimentation by Eggermann et al. Thus a calcium leak current was implemented as a source of calcium for  $i_{CAN}$ . In addition, the low-voltage activated  $i_T$  channels provide the

additional push of calcium for iCAN once iCal has provided its calcium stores. iCAN, in turn, is dependent on both voltage and calcium, and its reversal potential is not constant but a function of calcium concentration.

### *Limitations*

The model created shows a new understanding of the dynamics present in orexin neurons. There still are, however, many angles that have yet to be understood. Firstly, the neuron modeled lacks any synaptic interactions. The true dynamics of the neuron cannot be studied without the interactions it has with neighboring neurons that activate some of its currents. Therefore, further study is necessary to understand the true orexin neuron. In addition, it has been shown in experimental data that orexin neurons fire in clusters under certain circumstances. We did not address the mechanism involved in creating a rise in potential topped with sodium spikes.

### *Calcium*

The source of  $\text{Ca}^{2+}$  for iT and iCAN could be either a non-LVA current or a leak current from internal stores. We reviewed these possibilities and compared them with the activation of iCAN. The difference between the calcium from internal stores and calcium from leak is that the leak is consistently providing calcium regardless of the neuron's potential. iCAN needs to be more active at levels of lower potential so that iCAN can increase the neuron's potential to the point of spiking.

It is possible that a na/ca exchanger is also present in the neuron, but this possibility will require further study. The studies done on the sodium-calcium exchanger suggest that it is present not only in cardiac cells but in most cells in the body (Blaustein, Lederer, 1999). A calcium-sodium exchanger would fit in the model of orexin due to the presence of both sodium and calcium and also because it would provide another source of calcium for iCAN and iT while also using some of the large quantity of sodium present. A na/ca exchanger in orexin neurons would show interactions between two ions present in the neuron and would likely affect the resting membrane potential of the cell. However, the implementation of a na/ca exchanger would require a more complex study of the dynamics of both the cell and the exchanger.

### *Future Study*

The model as it stands supports vast growth in the study of orexin neurons. First, it is possible that the resting membrane potential is in fact more depolarized than we present here. How, though, would the depolarization block be lifted off a neuron so depolarized? Experimental results determining exactly which RMP is accurate would better allow modelers to pursue the correct dynamics of the system. Additionally, the graphs presented by Eggermann et al. are similar in shape to the ones created by the model, but it is difficult to match the two when it is not completely clear what the axes are on the graphs. With some tests, new graphs that are clearer would assist in modeling the activities of the neuron under various circumstances.

The canard oscillations introduce some interesting questions about the system. Is the spiking of an orexin neuron really an example of a canard? Careful measurements of  $\text{IK}_2$  and  $\text{iNa}$  could further describe what is happening during the interspike interval. This model is helpful for the future of working with orexin neuron because it provides a stepping stone for further experimentation.

## Works Cited

- Blaustein, M. P; Lederer, W. J. (1999). Sodium/Calcium Exchange: Its Physiological Implications. *Physiological Reviews*.
- Buchholtz, F; Golowasch, J; Epstein, I R; Marder, E. (1992). Mathematical Model of an Identified Stomatogastric Ganglion Neuron. *J. of Neurophysiology*. 332-340.
- Destexhe and Sejnowski (1993). A Model for 8-10 Hz Spindling in Interconnected Thalamic Relay and Reticularis Neurons. *Biophys J*. 2473-7.
- Eggermann, E; Bayer, L; Serafin, M; Sain-Mleux, B; Bernheim, L; Machard, D; Jones, B. E; Muhlethaler, M. (2003) The Wake-Promoting Hypocretin-Orexin Neurons Are in an Intrinsic State of Membrane Depolarization. *J. of Neuroscience*. 1557-1562.
- (Ermentrout, Bard. *Simulating, Analyzing, and Animating Dynamical Systems*. Philadelphia: SIAM, 2002
- Hoang, Q. V; Bajic, D; Yanagisawa, M; Nakajima, S; Nakajima, Y. (2003) Effects of Orexin (Hypocretin) on GIRK Channels. *J. of Neurophysiology*. 693-702.
- Huguenard, J. R; McCormick, D. A. (1992) Simulation of the Currents Involved in Rhythmic Oscillations in Thalamic Relay Neurons. *J. of Neurophysiology*. 1373-1383.
- Huguenard, J; McCormick, D. A. (1992). A Model of the Electrophysiological Properties of Thalamocortical Relay Neurons. *J. of Neurophysiology* 1384-1400.
- Izhikevich, E. M. *Dynamical Systems in Neuroscience*. Cambridge: MIT Press, 1976.
- Jalics, J; Krupa, M; Rotstein, H. G . (2008). A novel canard-based mechanism for mixed-mode oscillations in a neuronal model.
- Li, Y; Gao, X; Sakurai, T; van den Pol, A. N. (2002) Hypocretin/Orexin Excites Hypocretin Neurons via a Local Glutamate Neuron—A Potential Mechanism for Orchestrating the Hypothalamic Arousal System. *Neuron*. 1169-1181.
- McCormick, D. A; Bal, T. (1997). Sleep and Arousal: Thalamocortical Mechanisms. *Annu. Rev. Neuroscience*. 185-215.
- Murray, J. D. *Mathematical Biology: An Introduction*. New York: Springer, 2002.
- Sakurai, T. (2007) The neural circuit of orexin(hypocretin): maintaining sleep and wakefulness. *Neuroscience*. 171-181.